Thermochimica Acta 539 (2012) 23–33

Contents lists available at SciVerse ScienceDirect

Thermochimica Acta

journal homepage: www.elsevier.com/locate/tca

Quantitative kinetic and structural analysis of geopolymers. Part 1. The activation of metakaolin with sodium hydroxide

Zuhua Zhang[a,*], Hao Wang[a], John L. Provis[b], Frank Bullen[a], Andrew Reid[c], Yingcan Zhu[a]

[a] Faculty of Engineering and Surveying, University of Southern Queensland, Toowoomba, QLD, 4350, Australia
[b] Department of Chemical & Biomolecular Engineering, University of Melbourne, VIC, 3010, Australia
[c] Halok Pty Ltd., West End, QLD, 4101, Australia

ARTICLE INFO

Article history:
Received 8 January 2012
Received in revised form 20 March 2012
Accepted 23 March 2012
Available online 31 March 2012

Keywords:
Geopolymer
Isothermal conduction calorimetry
Metakaolin
Kinetics

ABSTRACT

Isothermal conduction calorimetry (ICC) is used here to measure the kinetics of geopolymerisation of metakaolin by reaction with NaOH solution under a variety of conditions. Three exothermic peaks are observed in the calorimetric curve, and are assigned to the dissolution of metakaolin, the formation of geopolymer with disordered or locally ordered structure, and finally the reorganization and partial crystallization of this inorganic polymer gels. For the purpose of further quantifying the ICC data, the geopolymeric reaction products are assumed to have an analcime-like local structure, and their standard formation enthalpies are estimated from the available data for this structure. This assumption enables ICC to be used for the first time in a quantitative manner to determine the real reaction kinetics of geopolymerization. Increasing the NaOH concentration up to a molar overall Na/Al ratio of 1.1 is seen to enhance the reaction extent observed at 3 days, up to a maximum of around 40% in the high liquid/solid ratio systems studied here, and accelerates the crystallization process. However, further addition of NaOH does not give any additional reaction within this period, or any further acceleration. Raising the reaction temperature from 25 °C to 40 °C increases the initial reaction rate but has little effect on the final reaction extent, particularly when Na/Al > 1.

1. Introduction

Geopolymer binders and cements are generally formed by reaction of an aluminosilicate powder (such as metakaolin or fly ash) with an alkaline solution. The chemical reaction process responsible for geopolymer formation, known as geopolymerization, involves the dissolution of Si and Al atoms from the source material, reorientation of precursor ions in solution, and condensation reactions to form an inorganic polymer (geopolymer) [1]. Since geopolymer production reduces the need for high temperature calcination processes compared with Portland cement clinker manufacture, geopolymers have high potential for use in 'green' concretes with less environmental impact than concretes based on ordinary Portland cement (OPC), particularly when local industrial wastes can be used [2]. In addition, geopolymers can possess other desirable properties such as high thermal shock resistance [3] and low permeability [4].

Extensive studies have been carried out to understand the effects of the type and concentration of alkaline activator on the process of geopolymerization and the mechanical properties of the final products [3,5–7]. To control properties such as the setting time and rheology of the geopolymer slurry, and to better understand the fundamental characteristics of the final products, detailed research related to reaction kinetics is essential [8]. Geopolymerization is a multistep process, involving dissolution, gel formation and transformation reactions involving crystallographically disordered phases, probably together with partial re-dissolution of the products as part of a dynamic equilibrium between gel and dissolved species [9]. This means that it is difficult to develop a characterization technique that can provide a unified and all-encompassing description of such a complex reaction sequence, although there have been various studies which have provided data characterizing different aspects of the reaction.

Calorimetry is a classic technique used in determining the reaction kinetics of cement [10]. It has also been introduced in studying alkali activation of slag [11], and in examining the effects of various parameters on alkali activation of metakaolin based geopolymers, such as reaction temperature [12–14], alkali type and concentration [12,15–18], and the nature of the starting kaolin/metakaolin precursor [19,20]. In these studies, which have applied both isothermal and non-isothermal measurements, the calorimetry provided helpful information regarding the process of geopolymerization, however, it has not previously been able to provide a quantitative determination of the real reaction extent,

* Corresponding author. Tel.: +61 7 46312549.
E-mail address: zuhua.zhang2@usq.edu.au (Z. Zhang).

0040-6031/$ – see front matter © 2012 Elsevier B.V. All rights reserved.
http://dx.doi.org/10.1016/j.tca.2012.03.021

Table 1
Composition of metakaolin (MK) as determined by XRF (wt.%; LOI is loss on ignition at 1000 °C).

Oxide	SiO_2	Al_2O_3	K_2O	MgO	Fe_2O_3	TiO_2	P_2O_5	Na_2O	LOI
Composition	55.57	41.55	0.43	0.05	0.56	0.26	0.23	0.26	0.91

similar to the information that can be obtained in OPC systems. This level of insight is able to be achieved for OPC because the hydration degree of OPC can be determined from the ratio of cumulative heat released to the total heat release expected at full hydration, which can be theoretically calculated [21]. Up to this time, the lack of a reliable measure of total heat release at 'full geopolymerization' has limited the use of calorimetry results in quantifying geopolymerization kinetics.

Alternative and novel characterization techniques have also provided useful information regarding the process of geopolymerization. Rees et al. [22] and Hajimohammadi et al. [23] used attenuated total reflectance Fourier transform infrared spectroscopy (ATR-FTIR) to monitor geopolymerization reaction systems at early age, providing the capability to monitor gel formation directly, but the application of this technique is often hindered by the presence of silica in the activating solution. Provis et al. [24–26] directly measured the reaction kinetics during the initial setting period by in situ energy-dispersive X-ray diffractometry (EDXRD) and alternating current impedance spectroscopy, and also presented a reaction kinetic model to describe the different stages of the reaction process. White et al. [27] developed a mathematical model for the process of geopolymer gel growth from metakaolin based on a coarse-grained Monte Carlo simulation using parameters derived from density functional theory, and also applied in situ neutron pair distribution function analysis to determine important information regarding structural evolution at early age [28], but quantification of the precise degree of reaction has also not yet been possible by these techniques.

It is clear that only a combination of multiple characterization techniques can give full insight into both the reaction extent and early-age products formed during geopolymerization. In this investigation, isothermal conduction calorimetry (ICC) is combined with X-ray diffraction (XRD), infrared spectroscopy (FTIR) and scanning electron microscopy (SEM) methods to monitor the geopolymerization process in the simplified metakaolin–NaOH system, and to examine the reaction products. Two important reaction parameters for geopolymerization – reaction temperature and alkali concentration – are investigated in terms of their influence on kinetics in a quantitative sense.

2. Experimental

2.1. Geopolymer paste formulation

The metakaolin (MK) used in this study was obtained by calcination of kaolin powder at 900 °C (Taojinfeng New Materials Co. Ltd., Fujian, China). Table 1 gives the composition of the MK as determined by X-ray fluorescence (XRF, Rh radiation). The particle size distribution is represented by the D_{10}, D_{50} and D_{90} values determined by laser diffraction, which were 1.4 μm, 5.9 μm, and 17.0 μm, respectively, and the specific surface area as measured by N_2 sorption and the Brunauer–Emmett–Teller (BET) method was 14.1 m^2/g. The activator used was sodium hydroxide solution, prepared by dissolving granular NaOH (chemical grade) in distilled water.

Table 2 gives the design of geopolymer pastes. It should be noted that the residual kaolinite (6.5 wt.% as calculated by assuming that the loss on ignition (LOI) of the metakaolin is due to the dehydration of kaolinite) is treated as part of the amorphous aluminosilicate content since it is also reactive; this assumption will be justified in Section 3 below. The quartz (estimated as 6.8 wt% by assuming all Al is from kaolinite, and that the kaolinite is 1:1 stoichiometric) is considered as being inactive in the geopolymerization process due to its low reactivity.

2.2. Calorimetry

The geopolymer pastes were studied in a 3114/3236 TAM 83 Air isothermal conduction calorimeter (Thermometric AB, Sweden) at 20, 25, 30, 35 and 40 °C by an internal mixing procedure. Preliminary tests showed that a homogeneous paste could be obtained by this procedure only when the liquid/solid ratio was higher than 0.8 mL/g for the calcined kaolin used in this study. The pastes studied were thus designed with a liquid/solid ratio of 1.0 mL/g to ensure successful mixing. The MK powder was placed in an ampoule containing a mini-blender, and NaOH solution was held separately in an injector. Both the ampoule and injector were maintained in the calorimeter at the reaction temperature until a thermal balance condition was reached. Once the NaOH activator was injected, the mini-blender was started and the heat flow immediately recorded at 10 s intervals. At each reaction temperature, the heat flow from a control paste prepared by mixing water with MK under the same conditions was also recorded, to provide a baseline to calibrate the result and to account for the heat due to wetting and the mini-blender. To minimize possible heat disturbances due to the environment, the room was maintained at the reaction temperature, except for the systems at 35 °C and 40 °C.

2.3. Characterization of geopolymers

After geopolymerization, a scanning electron microscope (JEOL Ltd., Japan) was used to analyze the morphology of selected specimens. Fracture surfaces were coated with gold, and imaged under high vacuum conditions with an accelerating voltage of 15 kV.

Powder samples were prepared for X-ray diffraction (XRD) and FTIR analysis by grinding the geopolymer reaction products in acetone followed by oven-drying at 65 °C for 6 h. The XRD analysis was conducted on an ARL 9900 Series X-ray workstation (Thermo Scientific) with Co K_α radiation operated at 40 kV and 40 mA at a scanning speed of 2.4° min^{-1}. The FTIR spectra were collected in the range 4000–400 cm^{-1} using a Nexus 670 FTIR spectrometer (Nicolet) in transmittance mode, with a sensitivity of 2 cm^{-1}. The spectra were converted into relative absorbance values, and deconvoluted in the range 800–1300 cm^{-1} using the Peakfit (Version 4.12) software with Gaussian peak shapes and variable peak widths. The fitting process, including setting the numbers and positions of component bands and adjusting the band shape, was performed in accordance with procedures described in the literature [22,29,30], combined with the self-fitting function of the software. The main principle used in the fitting procedure was to minimize the number of

Table 2
Composition of geopolymerization systems, defined as molar ratios.

NaOH (mol/L)	H_2O:Na	Na:Al	Al:Si
6	9.26	0.74	1
8	6.94	0.98	1
10	6.17	1.10	1
12	4.63	1.47	1

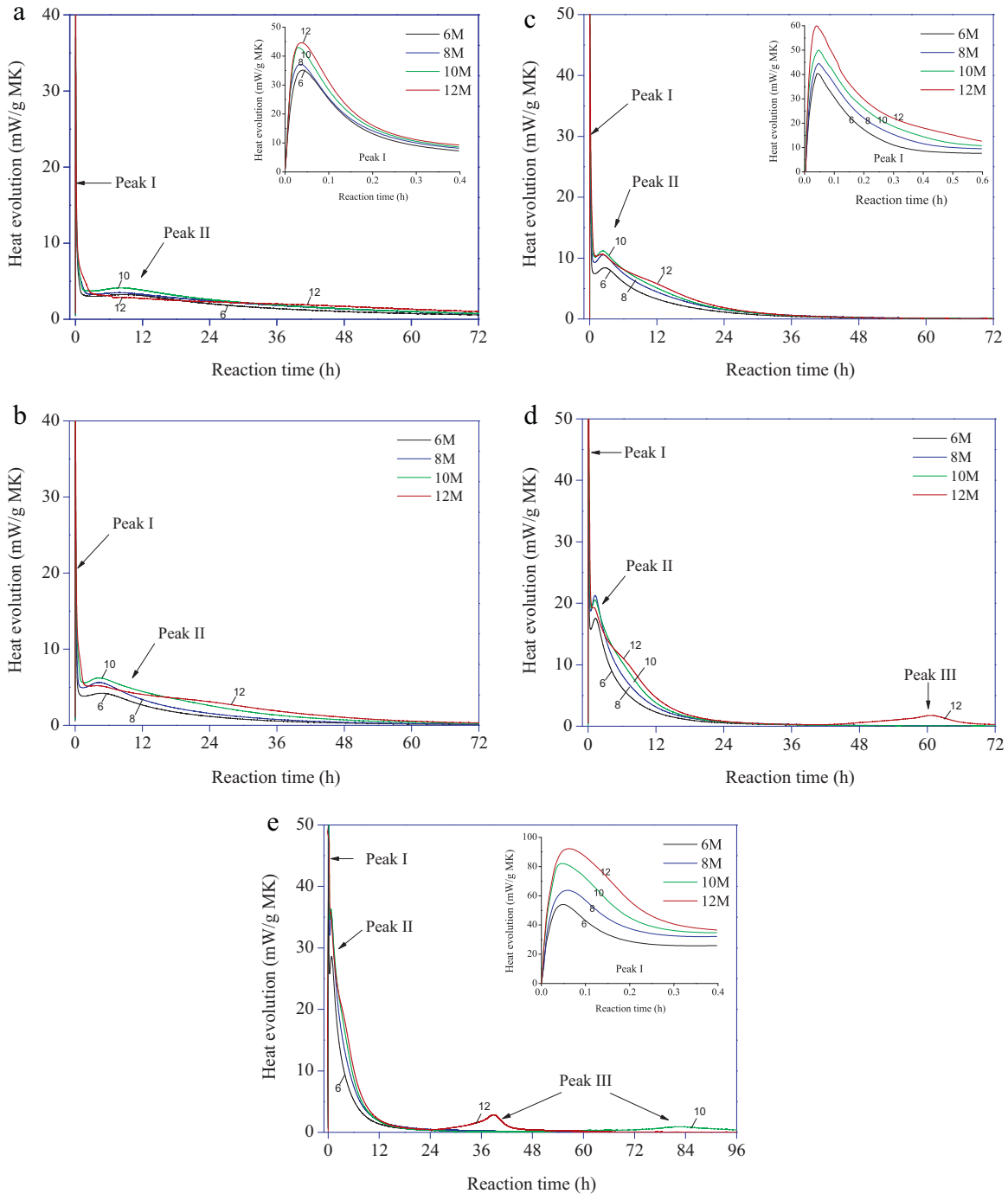

Fig. 1. Effects of NaOH concentration on heat evolution rate of MK geopolymerization at (a) 20 °C, (b) 25 °C, (c) 30 °C, (d) 35 °C and (e) 40 °C.

component bands while retaining a regression coefficient r^2 value above 0.999.

3. Results

3.1. ICC testing

Fig. 1 shows the heat evolution rates of MK activated with NaOH solution at 20–40 °C in the first 72 h of reaction. As mentioned in Section 2.2, the heat evolution rate data are corrected by subtracting the heat evolution of MK mixed with water, meaning that the data presented correspond specifically to the chemical reaction process.

In the reaction systems at 20–30 °C there are two distinct peaks in heat flow, as marked in Fig. 1: peak I is sharp and appears immediately after mixing, followed by a broad peak II. Peak III is only found in systems 12 M-35 °C (Fig. 1d), 12 M-40 °C and 10 M-40 °C (Fig. 1e), although it appears in the last of these after more than 72 h. The nature of the reaction processes responsible for each peak will be discussed below. The time required for peak I to reach a maximum in the rate of heat evolution is constant at around 5 min for all the systems studied, regardless of the reaction temperature. In contrast, the time corresponding to the maximum of peak II varies notably accordingly to the reaction temperature. Increasing the reaction temperature significantly shortens the time before the second maximum in heat evolution; this time period may be

Table 3
Cumulative heat release of exothermic peaks I and II in NaOH-activated metakaolin geopolymers in the first 72 h of reaction (or until the onset of peak III in some systems, where this time is noted).

NaOH (mol/L)	Heat release (J/g MK)				
	20 °C	25 °C	30 °C	35 °C	40 °C
6	461	326	414	436	442
8	544	421	541	556	578
10	588	580	584	622	626 (54 h)
12	571	625	624	655 (40.5 h)	656 (24 h)

compared with the 'induction period' observed in Portland cement hydration, although the physicochemical processes taking place will be very significantly different in geopolymerization. When viewed together with previous work [15], it is likely that there would also be a peak III in other systems with lower temperature and NaOH concentration, but that it would be weak, and would appear later than the 72-h period of the experiments here.

The amplitude of each heat release peak varies significantly as the reaction temperature is changed from 20 to 40 °C. For peak I, the maximum heat release rate increases monotonically with increasing NaOH concentration and temperature. For peak II, it is interesting to note that the maximum rate is usually higher in systems activated with 8 M or 10 M NaOH than in systems with a higher activator concentration of 12 M. This is attributed to the more extensive polymerization between Al and Si species taking place in the systems with slightly lower activator concentrations than at this highest alkalinity, as the solubility of aluminosilicate s increases with increasing pH; further discussion on this point will be presented later in this paper. The trend that the maximum heat evolution rate of peak II is much lower than peak I is consistent with the results of previous studies of metakaolin geopolymerization [15,31]. However, this trend can be altered by calcium addition [31], the use of a silicate activator [12] or the use of different aluminosilicate precursors [32].

The cumulative heat release of the first and second peaks in all systems is summarized in Table 3. The results fall in the same range as the systems measured by Alonso and Palomo [12] and by Muñiz-Villarreal et al. [13]. The slow reaction at 20 °C results in a higher total heat release than that at 25 °C in all systems except with 12 M NaOH. Higher NaOH concentrations or higher temperatures, being conditions which enhance the solubility of metakaolin, lead to a higher total heat release, as the dissolution of metakaolin is the most exothermic aspect of the reaction process, as seen qualitatively from the high early heat release (peak I) in all data sets in Fig. 1. Quantitative analysis in support of this attribution will be presented later in this paper.

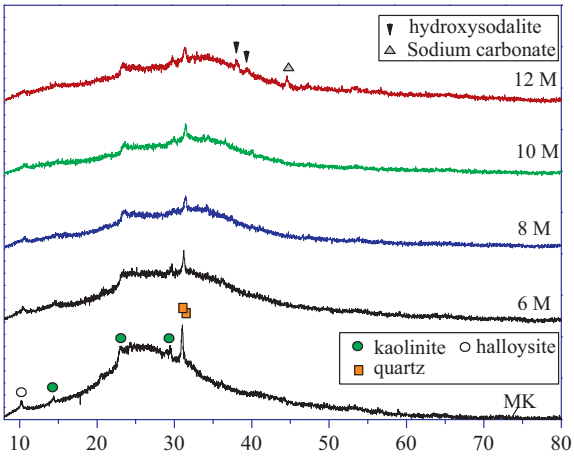

Fig. 2. Co Kα radiation XRD patterns of MK and its geopolymerization products after activation with NaOH solution of 6–12 mol/L at 30 °C for 72 h (kaolinite, $Al_2Si_2O_5(OH)_4$: powder diffraction file (PDF) #01-0527; halloysite, $Al_2Si_2O_5(OH)_4{\cdot}2H_2O$: PDF #09-0451; quartz, SiO_2: PDF #05-0490; hydroxysodalite, $Na_8Al_6Si_6O_{24}(OH)_2{\cdot}2H_2O$: PDF #46-1425; sodium carbonate, Na_2CO_3: PDF #1-1166).

3.2. XRD analysis

Fig. 2 shows the XRD data for MK and the geopolymer samples obtained after 72 h of reaction at 30 °C. The MK used is largely amorphous, with a small quantity of quartz as an impurity phase, and minor kaolinite and halloysite. The broad peak observed from 15 to 35° 2θ in MK has been broadened up to 40° 2θ after reaction with NaOH solution, with the center of gravity shifted to higher angle, as is well known to occur during geopolymer formation from metakaolin. This shift demonstrates the formation of new amorphous phases, usually described as geopolymeric gels [14,33]. The weakening of the diffraction peaks of kaolinite and halloysite (a tubular polymorph of kaolinite) suggests that these phases have participated in the reactions, which justifies their inclusion as reactive components in the mix design calculations in Section 2.1. In general the products are amorphous, and only in the 12 M system small amounts of hydroxysodalite (Powder Diffraction File (PDF) #46-1425) and sodium carbonate (PDF # 1-1166) are formed. The sodium carbonate may be formed due to carbonation of excess NaOH during sampling, crushing and XRD analysis. Comparing the relative intensities of the broad diffraction peaks in Fig. 2, the intensity between 30 and 40° 2θ (attributed to geopolymer) is seen to be higher than the intensity between 20 and 30° 2θ (attributed to MK) in the samples with higher NaOH concentration, implying increased formation of geopolymeric gels. This is particularly visible when comparing the intensities at around 33° 2θ and 27° 2θ in Fig. 2, where this ratio increases with NaOH concentration. However, the exact proportions of residual MK and newly formed gels are unable to be determined by XRD; this is an acknowledged shortcoming of this characterization method in analyzing materials with multiple distinct disordered ('X-ray amorphous') phases [24].

Fig. 3 shows the XRD patterns of the geopolymerization products from systems in which peak III appears (Fig. 1). Before peak III appears, for systems activated with NaOH concentration of 12 mol/L (Fig. 4a-36 h and b-18 h), the products are mainly amorphous. The small peaks appearing at 2θ = 28.16°, 31°, 34° and 35.04° are possibly due to crystalline nano-sized particles of zeolite A (PDF #39-0272); the same peaks were observed, but more intense and sharper, in the system with 10 mol/L at 40 °C (Fig. 4c-54 h), indicating a higher extent of crystallization and a larger crystallite size in this system. However, all systems studied contained predominantly disordered rather than crystalline aluminosilicate phases.

It is interesting to note that when comparing before and after peak III, the XRD patterns did not change significantly, indicating that this peak is not able to be attributed to a specific crystallization event in the gel systems. There is an increased diffraction intensity of zeolitic materials, but this is only slight, indicating that peak III is probably caused by reorganization within the polymer/zeolite precursor materials present, rather than a process of crystallization of more polymer gels. The distinct difference in the

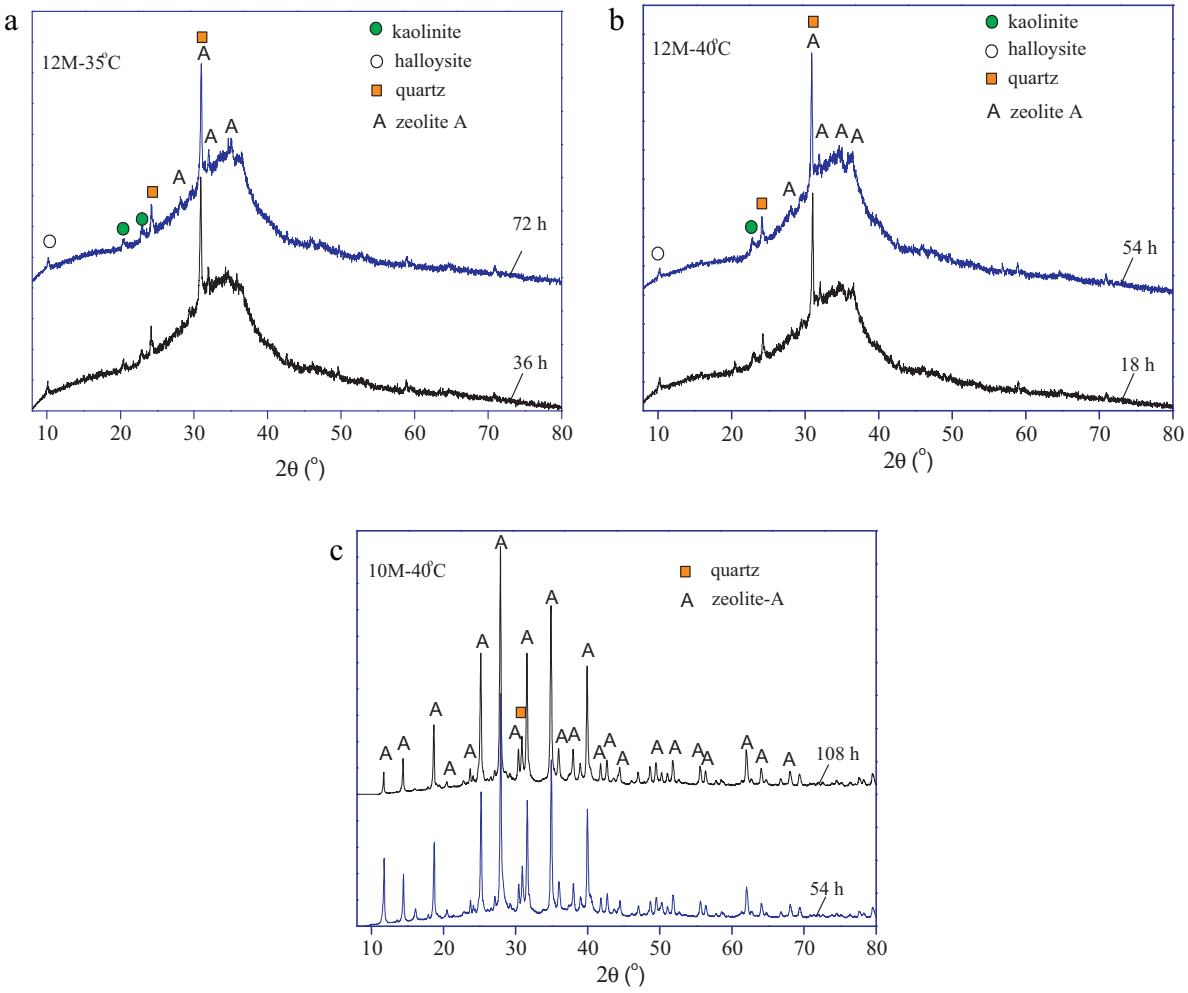

Fig. 3. Co Kα radiation XRD patterns of geopolymerization products of MK activated with NaOH solution for different periods: (a) 12 mol/L at 35 °C, (b) 12 mol/L at 40 °C and (c) 10 mol/L at 40 °C (zeolite A, $Na_{96}Al_{96}Si_{96}O_{384}{\cdot}216H_2O$: PDF #39-0272). Each of these systems shows a third exothermic peak in the isothermal calorimetry data ("peak III"), and each set of diffractograms contains one sample taken before the time of this peak, and another after the peak, with times as marked on the plots.

crystallinity of the products between the systems activated with 12 M NaOH compared to 10 M NaOH implies that zeolite phases preferred to form in systems with a slightly lower alkali content and higher reaction temperature. This may again be a solubility effect, or it may be because very high NaOH concentrations favor the formation of hydroxysodalite rather than zeolite A [34], and so the crystallization processes are slowed close to the phase boundary between these species. Although peak III is observed later in

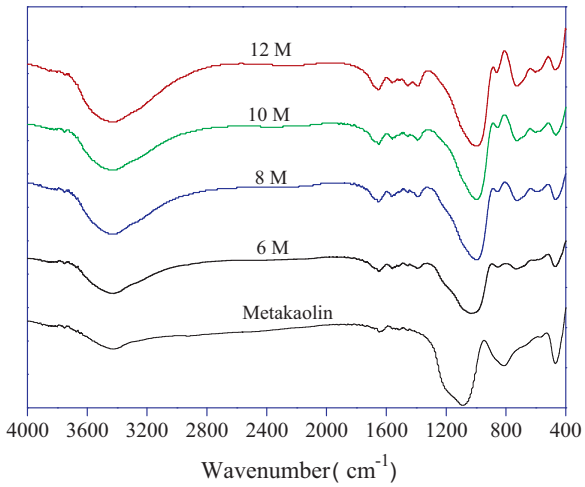

Fig. 4. FTIR spectra of MK and the geopolymerization products after activation with NaOH solution at 30 °C for 72 h.

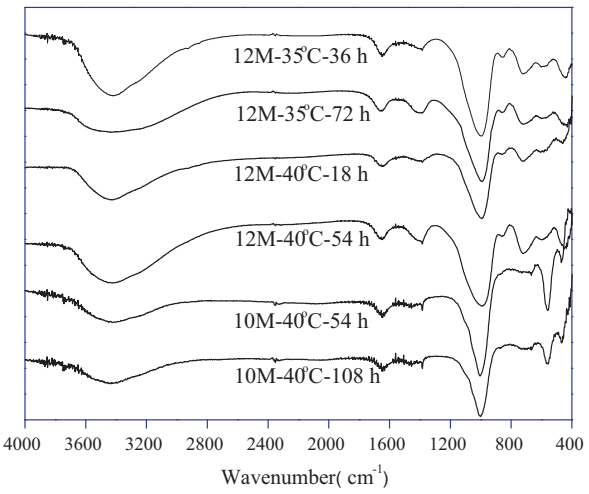

Fig. 5. FTIR spectra of selected geopolymerization products of MK activated with NaOH solution at 35 °C and 40 °C for different periods.

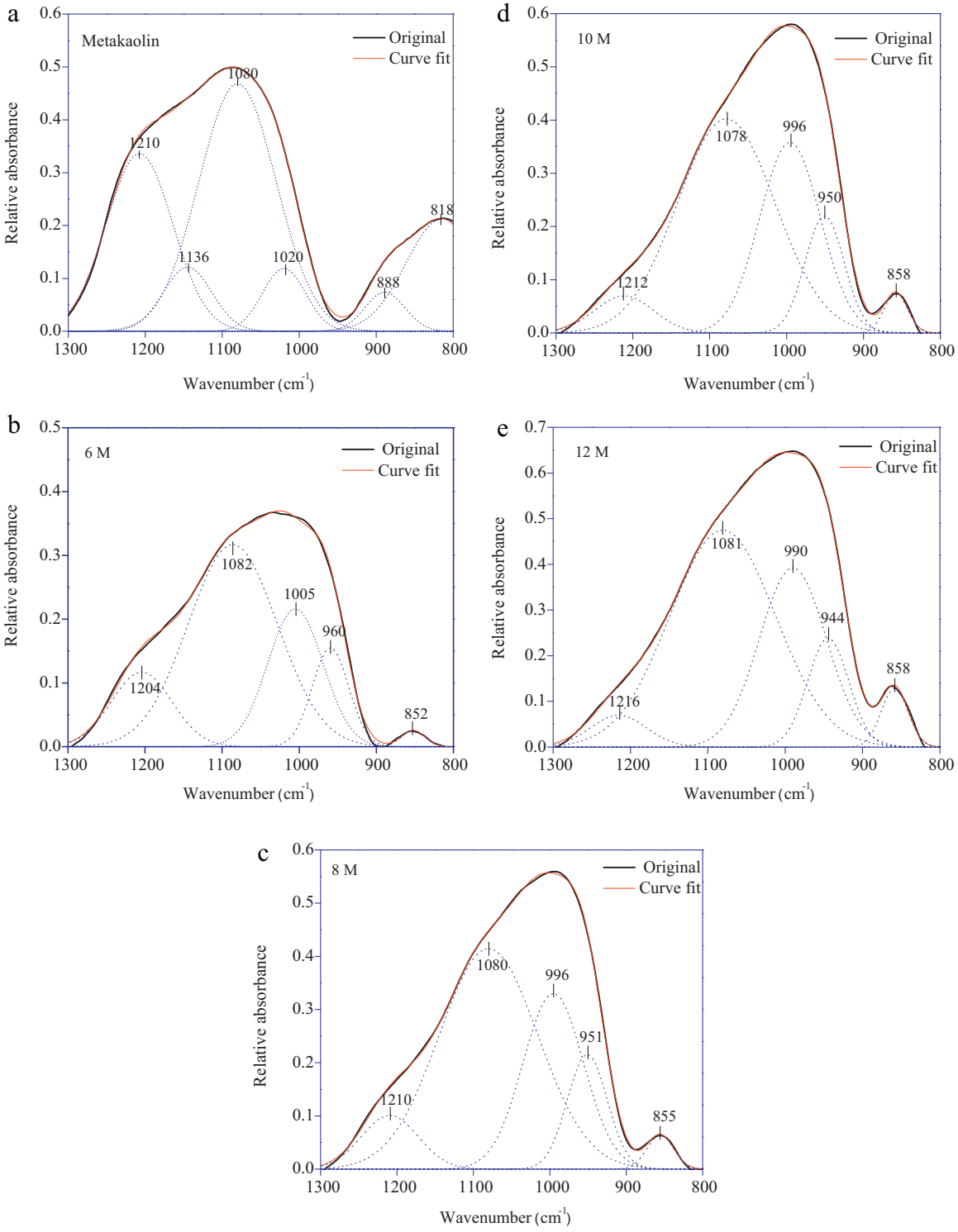

Fig. 6. FTIR spectral deconvolution of MK (a) and the geopolymerization products after activation with NaOH solution at 30 °C for 72 h: (b) 6 mol/L, (c) 8 mol/L, (d) 10 mol/L and (e) 12 mol/L.

the system with 10 M NaOH at 40 °C than in either of the 12 M NaOH systems shown in Fig. 3, comparison of the diffractograms obtained after 54 h in Fig. 3b and c shows a higher crystallinity at the same reaction time. There is much which remains to be understood regarding the kinetic and structural aspects of zeolite crystallization within geopolymers, as both kinetic and thermodynamic parameters influence phase relationships in these systems in complex ways, and there are almost always disordered and/or metastable phases formed.

3.3. FTIR analysis

The FTIR spectra of selected geopolymers are presented in Figs. 4 and 5. The most evident spectral differences are found

in the low-wavenumber region (400–800 cm^{-1}) and the middle-wavenumber region (800–1250 cm^{-1}).

In the low-wavenumber region, for the spectrum of MK (Fig. 4), the bands around 465 cm^{-1} are assigned to T—O (T = tetrahedral Al or Si) bending modes in TO_4 tetrahedra, and the band at 800 cm^{-1} is assigned to the Al—O bending mode of AlO_6 octahedra [17,35]. After geopolymerization, the intensities of these two bands both decrease, particularly at ~800 cm^{-1}, indicating the breakdown of the original octahedral structure of the residual kaolinite particles. The band at 710 cm^{-1} (Fig. 4) in the geopolymer spectra indicates the formation of Al^{IV} as the main Al environment in the polymer. The small band centered at ~600 cm^{-1} (Fig. 4) is probably caused by T—O vibrations in double rings in zeolite precursors [35]. A more prominent band at 557 cm^{-1} (Fig. 5) appears only in the systems 10 M-40 °C-54 h and 10 M-40 °C-108 h. This band is typically assigned to the external linkage vibrations of the TO_4 tetrahedra in the double rings of zeolite A [36], which agrees well with the XRD results.

In the mid-wavenumber region, a shift in the position of the broad Si—O—T asymmetric stretching peak (containing multiple overlapping components which sum to give a broad peak) from ~1080 cm^{-1} in MK to ~1000 cm^{-1} in the geopolymer product is observed, regardless of whether the product is entirely X-ray amorphous or contains a higher degree of crystalline material. This band shift is usually considered to be due to the formation of geopolymers [31,37], although it is also observed in the formation of zeolites from disordered aluminosilicate precursors [35,36].

The small band appearing at around 1440 cm^{-1} is related to the asymmetric stretching of the O—C—O bonds of CO_3^{2-} due to atmospheric carbonation on the surface of powdered products, which is only found within 12 M system for XRD pattern. The absorption bands at 1630–1660 cm^{-1}, combined with a very weak absorption band at around 3750 cm^{-1}, suggest the presence of isolated non-interacting surface silanol groups [38]. The increased intensity of bands at 1630–1660 and ~3400 cm^{-1} with increasing NaOH concentration implies that the activated products form with more surface hydroxyl groups hydrogen-bonded to adsorbed water (≡Si–OH···H_2O and ≡Al–OH···H_2O) in systems with higher alkali content. This is consistent with the common understanding that high pH favors depolymerization of aluminosilicates.

To obtain a better understanding of the causes of the band shift in the mid-wavenumber region, the spectra of products obtained at 30 °C in this range are enlarged and deconvoluted (see Section 2.3 for discussion of the deconvolution procedure) in Fig. 6. After alkali-activation of the metakaolin, the two new bands at 1005–990 cm^{-1} and 960–944 cm^{-1} are the most notable changes in the spectra. The principal new band at 1005–990 cm^{-1} is assigned to the asymmetric stretching vibration of Si–O–T links in geopolymer framework; this band is known to be sensitive to connectivity and Si/Al ratio [23], and in this case it is observed at a wavenumber consistent with the presence of predominantly Si–O–Al bonds, which agrees well with the stoichiometry of the systems studied. The second new band, at 960–944 cm^{-1}, is assigned to asymmetric stretching vibration of non-bridging oxygen sites, in particular Si–O–Na type structures [39,40]. Fig. 7 indicates the influence of the NaOH concentration on the positions of these two bands. With increasing NaOH concentration, both of these new bands shift to lower wavenumber. The shift in the Si–O–T component peak to lower wavenumber indicates a higher degree of conversion of Al from non-tetrahedral environments in metakaolin to tetrahedral environments bonded to Si in the geopolymer framework, which agrees well with the trends in extent of reaction of MK, and is also supported by findings in the literature for alkali-activated fly ash systems [40].

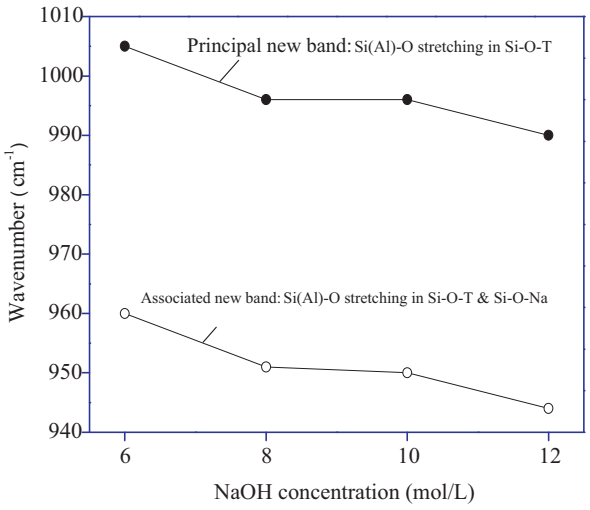

Fig. 7. The positions of the resolved principal new band and the associated new band in the FTIR deconvolutions of samples as a function of NaOH concentration.

3.4. SEM analysis

Fig. 8 exhibits micrographs of the fracture surfaces of geopolymerization products. Generally, after reaction with highly concentrated NaOH solutions, MK particles are converted into a porous, particulate gel, and are bound with each other on the surfaces or at the edge, but also maintain their plate-like morphology to some extent. The observed porous gel morphologies in this work are similar to previously published images of metakaolin geopolymers with low Si/Al ratios [41], and also resemble the precursor gels formed in some hydrothermal zeolite synthesis systems at very early stages [42].

Fig. 9 shows a fracture surface of the geopolymer obtained from system 10 M-40 °C. The distinct particles as marked by the arrows and emphasized in the circles in Fig. 9 are identified as being zeolite A crystallites, although these are still far from the perfect cubic crystal habit of pure zeolite A [35].

4. Modeling of geopolymerization kinetics

4.1. Geopolymerization process of NaOH-activated MK

Based on the calculated reaction enthalpy and the XRD and FTIR analysis presented in this study, a reasonable diagram relating the three exothermic peaks with three stages in reaction can be constructed as shown in Fig. 10, which is derived from the conceptual arguments which have previously been developed into a reaction kinetic model for geopolymerization [25,26,43].

In Stage I of the reaction process, the geopolymerization begins from the dissolution of metakaolin (MK) into silicate monomers (abbreviated S in the reaction scheme) and aluminate monomers (abbreviated A). In Stage II, the polymerization of S and A results in aluminosilicate oligomers (O), which immediately polymerize into small geopolymeric fragments (P) or 'proto-zeolitic nuclei' (N). P and N are thermodynamically metastable and incompletely cross-linked, and will assemble into aluminosilicate inorganic polymer gels (G) (approaching percolation of the network) and crystallized phases (Z), which are larger in molecular weight, higher in connectivity and more ordered in microstructure [25]. These two basic steps, O + S + A → P and/or N, and subsequently P and/or N → G and/or Z, overlap within the second broad exothermic peak in the ICC data, as the heat release involved in these processes has been calculated to be relatively low compared to the initial dissolution and oligomerization reactions [41]. From XRD and FTIR

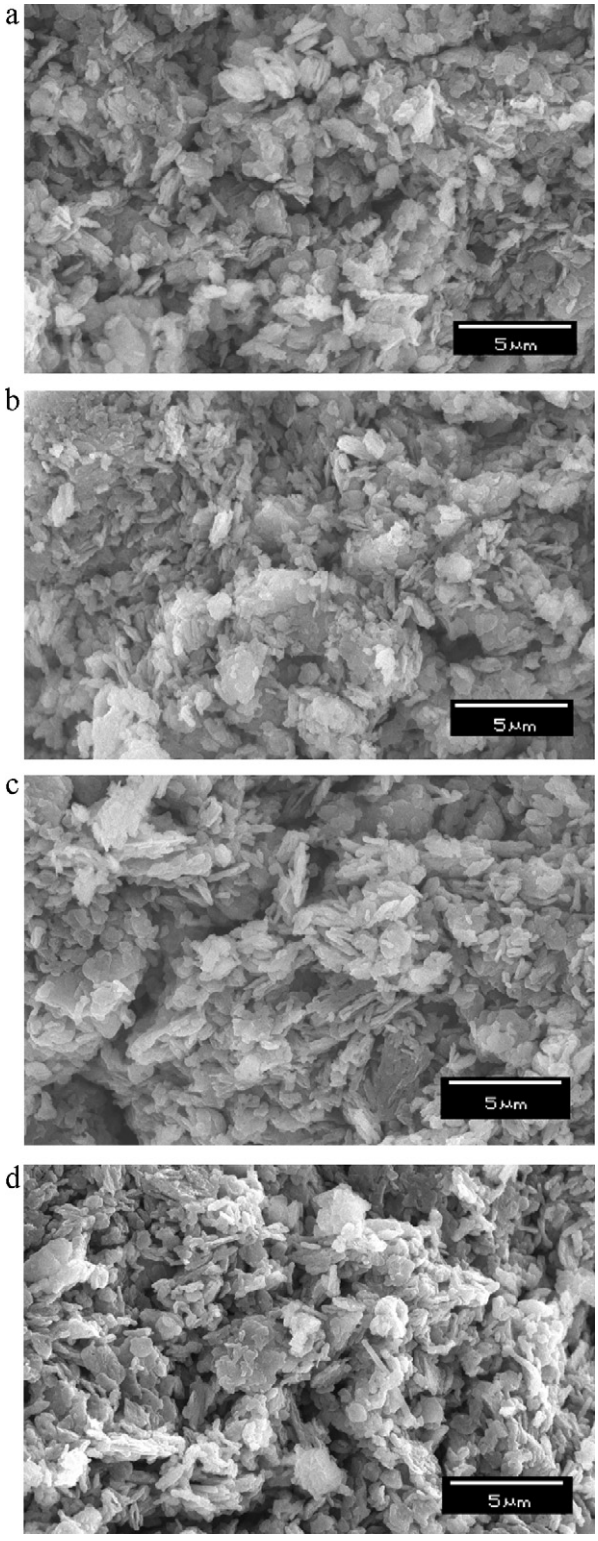

Fig. 8. SEM micrographs of the fracture surfaces of geopolymerization products of MK activated with NaOH solution: (a) 6 mol/L, (b) 8 mol/L, (c) 10 mol/L and (d) 12 mol/L.

analysis, phases consistent with both G (the disordered gels) and Z (crystalline zeolite) detectable in the reaction products obtained at 35 or 40 °C, at the end of Stage II of the reaction (Fig. 3). The final exothermic peak, in Stage III of the reaction, is thus related to two possible transformations: the crystallization of G into Z; and the further reorganization of G and/or Z into other more

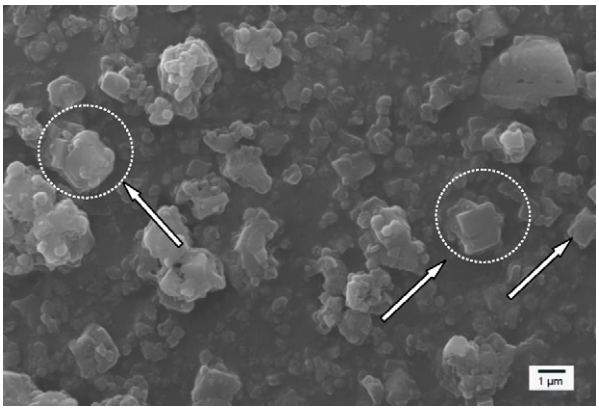

Fig. 9. SEM micrograph of the surface of the geopolymerization products of system 10 M-40 °C after 54 h of reaction. Circles and arrows mark products which are similar in morphology to zeolite A crystallites.

cross-linked and thermodynamically stable states. If the former is true, there should be some zeolites detectable in the systems 12 M-35 °C-72 h and 12 M-40 °C-54 h which were not present in these systems prior to this heat release peak. However, neither XRD nor FTIR indicates that any notable quantity of zeolite is formed during this heat evolution peak. The reorganization of G seems more reasonable, possibly including reactions between the disordered polymers to form proto-zeolitic nuclei [44] which are too small to be detected by XRD. The transformation of a geopolymer from an initial amorphous state to a final amorphous state without notable development of crystallinity has been observed a number of times in the literature [1,24,28], and so this is likely to be the explanation for the occurrence of the third exothermic peak.

4.2. Quantification of geopolymerization kinetics

4.2.1. Thermodynamics of G and Z

An isothermal conduction calorimetry measurement supplies information regarding the reaction enthalpy during the geopolymerization process as described in Section 4.1. To use the ICC data to quantify the extent of geopolymerization, the determination of the thermodynamic parameters of G and Z is critical. However, due to the absence of existing high-quality thermodynamic data, and the difficulty in measuring the thermodynamic parameters through experiments from system to system, the thermodynamic parameters of G and Z can only be estimated at present. The estimation procedure used here provides significant advances over previous work aimed at estimating these parameters [43], because the use of pair distribution function has shown that metakaolin-derived geopolymer binders show very similar local (<6 Å) structures to

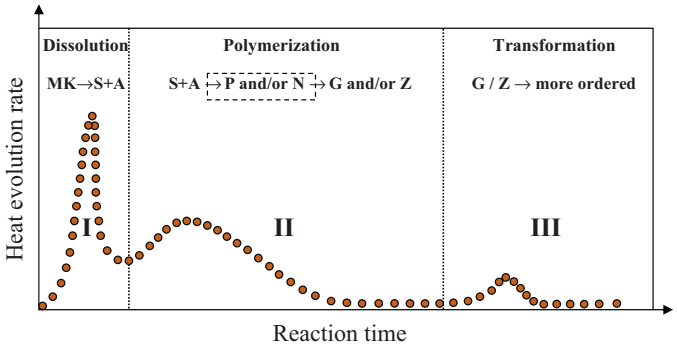

Fig. 10. Schematic of the kinetics of geopolymer synthesis by NaOH activation of MK, as determined by isothermal calorimetry.

zeolites of the analcime family—leucite for K-geopolymers [45,46], and pollucite for Cs-geopolymers [47], meaning that this well-understood mineral structure is now able to be used as a model for thermochemical calculations.

4.2.2. An assumption is thus raised for the estimation as follows

G and Z are the geopolymerization products with an approximate composition of $M^+[AlO_2{\cdot}nSiO_2]^-{\cdot}wH_2O$ (with n close to 1 for the systems studied here, but variable depending on the starting materials), in which the AlO_4 and SiO_4 tetrahedra link in Q^4 analcime-like structures when viewed at short range. The standard formation enthalpies of G and Z are assumed to be similar, as it has been shown that the energetics of crystalline and non-crystalline alkali aluminosilicates are very similar [48]. Thus, these values can be calculated using the standard enthalpies of formation of analcime ($[NaAlSi_2O_6]{\cdot}H_2O$) and amorphous glass (SiO_2), i.e.:

$$\Delta H^0_{f,298(G\ \text{or}\ Z)} = \Delta H^0_{f,298}(\text{analcime}) + (n-2)\cdot\Delta H^0_{f,298}(\text{amorphous SiO}_2) \quad (1)$$

where $\Delta H^0_{f,298}(\text{analcime}) = -3303.2$ kJ/mol [49], and $\Delta H^0_{f,298}(\text{amorphous SiO}_2) = -904.2$ kJ/mol [50].

Although the zeolite crystallites observed in this study are in fact zeolite Na–A rather than analcime, such zeolites are commonly observed in many other studies of geopolymer synthesis [30,51], and as mentioned above, the local structure of several geopolymers has been found to resemble zeolites of this family. Additionally, the thermochemical data available for analcime are considered reliable, whereas data for zeolite A are scarce. The content of structural H_2O in a zeolite also obviously has an effect on its standard formation enthalpy [52]. The content of structural (chemically bound) H_2O in geopolymeric gels has been found to be between 4 and 10 wt.% [53–56], depending on the raw materials and the reaction conditions. However, in this study and with the purpose of simplifying the calculations, it is assumed to be fixed with a molar ratio of H_2O to AlO_4 set equal to 1.

Accordingly, the whole process of NaOH activating MK to form (via a multi-step process) G and Z, can be simplified into a single overall equation:

$$Al_2O_3{\cdot}2SiO_2 + 2OH^- + 2Na^+ + H_2O \rightarrow 2NaAlSiO_4{\cdot}H_2O \quad (2)$$

Here the dissolution of Si and Al from MK is assumed to be stoichiometric. With the standard enthalpies of MK ($Al_2O_3{\cdot}2SiO_2$) (−3213.4 kJ/mol) [57], OH^- (−230.0 kJ/mol) [50], Na^+ (−240.3 kJ/mol) [50] and H_2O (−285.8 kJ/mol) [50], the reaction enthalpy of Eq. (2) at 298 K is estimated to be −358.2 kJ/mol (−1612.4 J/g) MK. If the 'general' reaction extent α is then defined as the ratio of the experimental heat release at any point in time to this theoretical maximum heat release at full reaction, the extent of reaction during the geopolymerization of NaOH-activated MK can now for the first time be quantified by calorimetry.

4.3. Effects of NaOH concentration and temperature on the reaction extent

Fig. 11 shows the effect of NaOH concentration on the reaction extent α. When Na/Al is <1, increasing NaOH concentration is effective in increasing the reaction extent. Although using ICC to determine the reaction extent may be considered to some degree an approximate method, the reaction extent α obtained is reasonable, according to the FTIR deconvolution analysis in Fig. 6. If it is assumed that the resolved bands at 1204–1215 and 1078–1086 cm^{-1} are assigned to the Si–O–T vibration in the incompletely dissolved MK present within the geopolymer, and their relative areas are proportional to their quantities (Fig. 12),

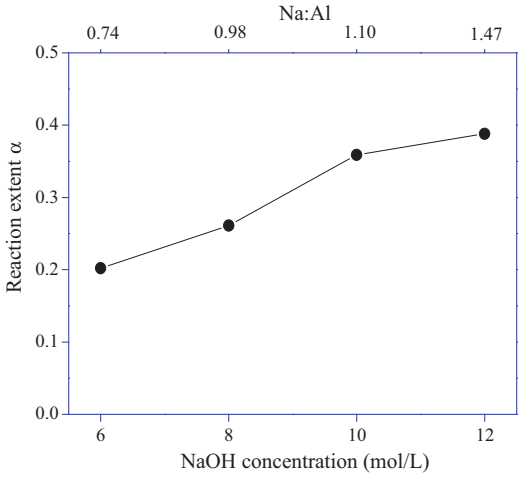

Fig. 11. The reaction extent of geopolymerization systems at 25 °C.

the incompletely dissolved MK comprises 70% of the system with 6 mol/L NaOH at 30 °C, and 60% at 12 mol/L NaOH and 30 °C. Thus, the ICC results agree very well with the FTIR deconvolution analysis. Granizo and Blanco [18] reported a reaction extent of around 50% when MK was activated with NaOH solution (12 mol/L) at 35–45 °C; the higher reaction extent of their metakaolin is likely to be due to the higher temperature and the higher specific surface area of their MK particles than those used here.

Fig. 13 shows the effects of reaction temperature on the reaction extent, which is calculated from the ICC data based on the assumption that the reaction enthalpy of Eq. (2) is constant at −358.2 kJ/mol within the temperature range of interest here. Since stage II of the reaction has not been completed within 72 h at 20 °C, only systems at temperatures of 25–40 °C are compared. When Na/Al = 0.98, raising the temperature from 25 to 30 °C gives an increase in the fractional reaction extent from 0.26 to 0.33. However, further raising the temperature to 40 °C only achieves another 0.03 increase in reaction extent. For systems with Na/Al = 1.10, the reaction extent only increases from 0.36 to 0.40 when changing the temperature from 25 to 40 °C. This means that for a metakaolin with a given specific surface area, when activated with NaOH at Na/Al > 1, varying reaction temperature can change the reaction rate significantly but has only a very slight influence on its reaction extent.

The above results and analysis have demonstrated that ICC is a powerful technique in studying the process of geopolymerization as it gives real-time heat exchange information from metakaolin

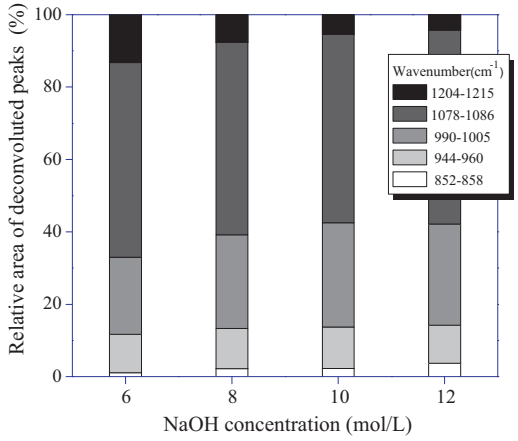

Fig. 12. Relative area of the deconvoluted component peaks in the main Si–O–T vibration band region (800–1300 cm^{-1}) in geopolymer samples.

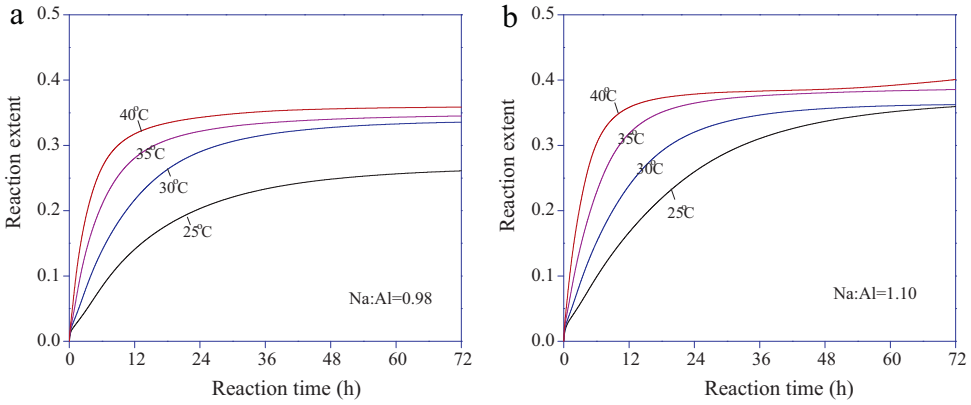

Fig. 13. Effects of reaction temperature on the reaction extent in geopolymer systems as represented by the cumulative heat of reaction: (a) Na:Al = 0.98; (b) Na:Al = 1.10.

particles contacting the activator. Based on the assumptions of the thermodynamic parameters of the reaction products, ICC can further quantify the reaction kinetics and thus determine the reaction extent of metakaolin particles. The effects of some important factors, such as alkali concentration and reaction temperature, on the kinetics can be qualified by this methodology. Further investigations into more complex systems will be performed in subsequent publications, such as for sodium silicate activation of metakaolin.

5. Conclusions

The geopolymerization process and early-age reaction products of NaOH-activated metakaolin, reacted at 20–40 °C, have been studied by the use of isothermal conduction calorimetry combined with structural and microscopic analysis. The calorimetric curves show either two or three distinguishable exothermic peaks after the metakaolin is mixed with the NaOH solution. The first sharp peak corresponds to the dissolution of metakaolin, and the second is associated with the polymerization of dissolved species together with the transformation of freshly formed oligomeric and/or polymeric products into fully cross-linked frameworks and/or zeolitic products. The degree of crystallinity is enhanced by increasing temperature, but not always by increasing the NaOH concentration, due to the higher solubility of aluminosilicates at very high alkalinity. In samples which are sufficiently reactive to partially crystallize (either as moderately large crystallites or as partially ordered pseudo-zeolitic structures), a third exothermic peak is observed, which is attributed to the further reorganization of the solid structures into a more stable (although not necessarily notably more crystalline) state. Low reaction temperatures reduce the formation of zeolite phases.

Based on this mechanistic insight, and making use of the fact that the geopolymer binder structure is known to be similar to that of analcime-group minerals on a nanoscale level, the reaction extent of geopolymerization has been quantified from the isothermal conduction calorimetry data. Fractional reaction extents of up to 0.4 are observed at 72 h after mixing, and the results of deconvolution of infrared spectra are consistent with the values obtained from the calorimetric data. Increasing the NaOH concentration from Na/Al = 0.74 to 1.10 leads to an increase in the reaction extent. However, the addition of more NaOH beyond this point is not helpful in improving the reaction extent or shortening the main reaction period as indicated by the time at which the first two peaks are observed. Raising the reaction temperature from 25 °C to 40 °C accelerates the reaction, but shows little effect on the final reaction extent, particularly when Na/Al > 1. The methodology developed here shows good potential in providing an accurate measure of the extent of reaction of metakaolin-based geopolymer systems, a goal which has remained largely elusive to date, and will be further developed in the future to the analysis of more complex geopolymer systems, including those with silicate activating solutions.

Acknowledgements

ZZ thanks Chen Y. and Yang T. (NJUT) for their technical assistance in ICC measurement and XRD characterization. The participation of JLP was funded by the Australian Research Council, including partial funding through the Particulate Fluids Processing Centre.

References

[1] P. Duxson, A. Fernández-Jiménez, J.L. Provis, G.C. Lukey, A. Palomo, J.S.J. van Deventer, Geopolymer technology: the current state of the art, J. Mater. Sci. 42 (2007) 2917–2933.
[2] B.C. McLellan, R.P. Williams, J. Lay, A. van Riessen, G.D. Corder, Costs and carbon emissions for geopolymer pastes in comparison to ordinary Portland cement, J. Cleaner Prod. 19 (2011) 1080–1090.
[3] A.M. Rashad, S.R. Zeedan, The effect of activator concentration on the residual strength of alkali-activated fly ash pastes subjected to thermal load, Constr. Build. Mater. 25 (2011) 3098–3107.
[4] Z. Zhang, X. Yao, H. Zhu, Potential application of geopolymers as protection coatings for marine concrete. I. Basic properties, Appl. Clay Sci. 49 (2010) 1–6.
[5] J.W. Phair, J.S.J. van Deventer, Effect of silicate activator pH on the leaching and materials characteristics of waste-based inorganic polymers, Miner. Eng. 14 (2001) 289–304.
[6] U. Rattanasak, P. Chindaprasirt, Influence of NaOH solution on the synthesis of fly ash geopolymer, Miner. Eng. 22 (2009) 1073–1078.
[7] E. Álvarez-Ayuso, X. Querol, F. Plana, A. Alastuey, N. Morenoa, M. Izquierdo, O. Font, T. Morenoa, S. Diez, E. Vázquez, M. Barra, Environmental, physical and structural characterisation of geopolymer matrixes synthesised from coal (co-)combustion fly ashes, J. Hazard. Mater. 154 (2008) 175–183.
[8] J.L. Provis, C.A. Rees, Geopolymer synthesis kinetics, in: J.L. Provis, J.S.J. van Deventer (Eds.), Geopolymers: Structure, Processing, Properties and Industrial Applications, Woodhead Publishing, Abingdon, UK, 2009, pp. 118–136.
[9] T. Ejaz, A.G. Jones, P. Graham, Solubility of zeolite A and its amorphous precursor under synthesis conditions, J. Chem. Eng. Data 44 (1999) 574–576.
[10] J.I. Bhatty, A review of the applications of thermal analysis to cement–admixture systems, Thermochim. Acta 189 (1991) 313–350.
[11] A. Fernández-Jiménez, F. Puertas, A. Arteaga, Determination of kinetic equations of alkaline activation of blast furnace slag by means of calorimetric data, J. Therm. Anal. 52 (1998) 945–955.
[12] S. Alonso, A. Palomo, Alkaline activation of metakaolin and calcium hydroxide mixtures: influence of temperature, activator concentration and solids ratio, Mater. Lett. 47 (2001) 55–62.
[13] M.S. Muñiz-Villarreal, J.L. Reyes-Araiza, S. Sampieri-Bulbarela, J.R. Gasca-Tirado, A. Manzano-Ramírez, J.C. Rubio-Ávalos, J.J. Pérez-Bueno, L.M. Apatiga, A.Z. Cadena, V. Amigó-Borrás, The effect of temperature on the geopolymerization process of a metakaolin-based geopolymer, Mater. Lett. 65 (2011) 995–998.
[14] H. Rahier, B. van Mele, M. Biesemans, J. Wastiels, X. Wu, Low-temperature synthesized aluminosilicate glasses. 1. Low-temperature reaction stoichiometry and structure of a model compound, J. Mater. Sci. 31 (1996) 71–79.
[15] X. Yao, Z. Zhang, H. Zhu, Y. Chen, Geopolymerization process of alkali-metakaolinite characterized by isothermal calorimetry, Thermochim. Acta 493 (2009) 49–54.

[16] A. Buchwald, R. Tatarin, D. Stephan, Reaction progress of alkaline-activated metakaolin-ground granulated blast furnace slag blends, J. Mater. Sci. 44 (2009) 5609–5617.
[17] H. Rahier, W. Simons, B. Van Mele, M. Biesemans, Low-temperature synthesized aluminosilicate glasses. 3. Influence of the composition of the silicate solution on production, structure and properties, J. Mater. Sci. 32 (1997) 2237–2247.
[18] M.L. Granizo, M.T. Blanco, Alkaline activation of metakaolin. An isothermal conduction calorimetry study, J. Therm. Anal. 52 (1998) 957–965.
[19] M.L. Granizo, M.T. Blanco-Varela, A. Palomo, Influence of the starting kaolin on alkali-activated materials based on metakaolin. Study of the reaction parameters by isothermal conduction calorimetry, J. Mater. Sci. 35 (2000) 6309–6315.
[20] H. Rahier, J.F. Denayer, B. van Mele, Low-temperature synthesized aluminosilicate glasses. Part IV. Modulated DSC study on the effect of particle size of metakaolinite on the production of inorganic polymer glasses, J. Mater. Sci. 38 (2003) 3131–3136.
[21] I. Pane, W. Hansen, Investigation of blended cement hydration by isothermal calorimetry and thermal analysis, Cem. Concr. Res. 35 (2005) 1155–1164.
[22] C.A. Rees, J.L. Provis, G.C. Lukey, J.S.J. van Deventer, In situ ATR-FTIR study of the early stages of fly ash geopolymer gel formation, Langmuir 23 (2007) 9076–9082.
[23] A. Hajimohammadi, J.L. Provis, J.S.J. van Deventer, Time-resolved and spatially-resolved infrared spectroscopic observation of seeded nucleation controlling geopolymer gel formation, J. Colloid Interface Sci. 357 (2011) 384–392.
[24] J.L. Provis, J.S.J. van Deventer, Geopolymerisation kinetics. 1. In situ energy-dispersive X-ray diffractometry, Chem. Eng. Sci. 62 (2007) 2309–2317.
[25] J.L. Provis, J.S.J. van Deventer, Geopolymerisation kinetics. 2. Reaction kinetic modeling, Chem. Eng. Sci. 62 (2007) 2318–2329.
[26] J.L. Provis, P.A. Walls, J.S.J. van Deventer, Geopolymerisation kinetics. 3. Effects of Cs and Sr salts, Chem. Eng. Sci. 63 (2008) 4480–4489.
[27] C.E. White, J.L. Provis, T. Proffen, J.S.J. van Deventer, Molecular mechanisms responsible for the structural changes occurring during geopolymerization: multiscale simulation, AIChE J., http://dx.doi.org/10.1002/aic.12743, in press.
[28] C.E. White, J.L. Provis, A. Llobet, T. Proffen, J.S.J. van Deventer, Evolution of local structure in geopolymer gels: an in situ neutron pair distribution function analysis, J. Am. Ceram. Soc. 94 (2011) 3532–3539.
[29] P. Rovnaník, Effect of curing temperature on the development of hard structure of metakaolin-based geopolymer, Constr. Build. Mater. 24 (2010) 1176–1183.
[30] D. Akolekar, A. Chaffee, F.H. Russell, The transformation of kaolin to low-silica X-zeolite, Zeolites 19 (1997) 359–365.
[31] M.L. Granizo, S. Alonso, M.T. Blanco-Varela, A. Palomo, Alkaline activation of metakaolin. Effect of calcium hydroxide in the products of reaction, J. Am. Ceram. Soc. 85 (2002) 225–231.
[32] S. Kumar, R. Kumar, S.P. Mehrotra, Influence of granulated blast furnace slag on the reaction, structure and properties of fly ash based geopolymer, J. Mater. Sci. 45 (2010) 607–615.
[33] A. Hajimohammadi, J.L. Provis, J.S.J. van Deventer, The effect of silica availability on the mechanism of geopolymerization, Cem. Concr. Res. 41 (2011) 210–216.
[34] R.M. Barrer, D.E. Mainwaring, Chemistry of soil minerals. Part XIII. Reactions of metakaolinite with single and mixed bases, J. Chem. Soc. Dalton Trans. 22 (1972) 2534–2546.
[35] C.A. Ríos, C.D. Williams, M.A. Fullen, Nucleation and growth history of zeolite LTA synthesized from kaolinite by two different methods, Appl. Clay Sci. 42 (2009) 446–454.
[36] M. Alkan, C. Hopa, Z. Yilmaz, H. Guler, The effect of alkali concentration and solid/liquid ratio on the hydrothermal synthesis of zeolite NaA from natural kaolinite, Microporous Mesoporous Mater. 86 (2005) 176–184.
[37] Y. Zhang, W. Sun, Z. Li, Infrared spectroscopy study of structural nature of geopolymeric products, J. Wuhan Univ. Technol. 23 (2008) 522–527.
[38] I. Giannopoulou, D. Panias, Hydrolytic stability of sodium silicate gels in the presence of aluminum, J. Mater. Sci. 45 (2010) 537–5377.
[39] S.A. Bernal, J.L. Provis, V. Rose, R. Mejía de Gutiérrez, Evolution of binder structure in sodium silicate-activated slag-metakaolin blends, Cem. Concr. Compos. 33 (2011) 46–54.
[40] W.K.W. Lee, J.S.J. van Deventer, Use of infrared spectroscopy to study geopolymerization of heterogeneous amorphous aluminosilicates, Langmuir 19 (2003) 8726–8734.
[41] P. Duxson, J.L. Provis, G.C. Lukey, S. Mallicoat, W.M. Kriven, J.S.J. van Deventer, Understanding the relationship between geopolymer composition microstructure and mechanical properties, Colloids Surf., A 269 (2005) 47–58.
[42] S. Chandrasekhar, P.N. Pramada, Microwave assisted synthesis of zeolite A from metakaolin, Microporous Mesoporous Mater. 108 (2008) 152–161.
[43] J.L. Provis, P. Duxson, J.S.J. van Deventer, G.C. Lukey, The role of mathematical modelling and gel chemistry in advancing geopolymer technology, Chem. Eng. Res. Des. 83 (A7) (2005) 853–860.
[44] S. Mintova, N.H. Olson, V. Valtchev, T. Bein, Mechanism of zeolite A nanocrystal growth from colloids at room temperature, Science 283 (1999) 958–960.
[45] J.L. Bell, P. Sarin, P.E. Driemeyer, R.P. Haggerty, P.J. Chupas, W.M. Kriven, X-ray pair distribution function analysis of a metakaolin-based, $KAlSi_2O_6{\cdot}5.5H_2O$ inorganic polymer (geopolymer), J. Mater. Chem. 18 (2008) 5974–5981.
[46] C.E. White, J.L. Provis, T. Proffen, J.S.J. van Deventer, The effects of temperature on the local structure of metakaolin-based geopolymer binder: a neutron pair distribution function investigation, J. Am. Ceram. Soc. 93 (2010) 3486–3492.
[47] J.L. Bell, P. Sarin, J.L. Provis, R.P. Haggerty, P.E. Driemeyer, P.J. Chupas, J.S.J. van Deventer, W.M. Kriven, Atomic structure of a cesium aluminosilicate geopolymer: a pair distribution function study, Chem. Mater. 20 (2008) 4768–4776.
[48] A. Navrotsky, Z.R. Tian, Sytematics in the enthalpies of formation of anhydrous aluminosilicate zeolite, glass and dense phases, Chem. Eur. J. 7 (2001) 769–774.
[49] P.S. Neuhoff, G.L. Hovis, G. Balassone, J.F. Stebbins, Thermodynamic properties of analcime solid solutions, Am. J. Sci. 304 (2004) 21–66.
[50] Common Thermodynamic Database Project, http://www.ctdp.org/#http%3A//www.ctdp.org/ctd_import/species_list/species_3785/view [25.08.2011].
[51] J. Wang, C. Han, J. Wang, Y. Li, Y. Teng, X. Wu, Composition and microstructure of 'alkali-slag-coal fly ash-metakaolin' hydroceramics, J. Chin. Ceram. Soc. 39 (2011) 512–517.
[52] G.K. Johnson, H.E. Flotow, P.A.G. O'Hare, W.S. Wise, Thermodynamic studies of zeolites: analcime and dehydrated analcime, Am. Miner. 67 (1982) 736–748.
[53] D. Dimas, I. Giannopoulou, D. Panias, Polymerization in sodium silicate solutions: a fundamental process in geopolymerization technology, J. Mater. Sci. 44 (2009) 3719–3730.
[54] Z. Zhang, X. Yao, H. Zhu, Y. Chen, Role of water in the synthesis of calcined kaolin-based geopolymer, Appl. Clay Sci. 43 (2009) 218–223.
[55] D.L.Y. Kong, J.G. Sanjayan, K. Sagoe-Crentsil, Factors affecting the performance of metakaolin geopolymers exposed to elevated temperatures, J. Mater. Sci. 43 (2008) 824–831.
[56] V. Živica, S. Balkovic, M. Drabik, Properties of metakaolin geopolymer hardened paste prepared by high-pressure compaction, Constr. Build. Mater. 25 (2011) 2206–2213.
[57] N.C. Schieltz, M.R. Soliman, Thermodynamics of the various high temperature transformations of kaolinite, in: Proceedings of the 13th National Conference on Clays and Clay Minerals, Pergamon Press, New York, 1966, pp. 419–428.